Progetto di sviluppo concessione "Colle Santo"

Procedura di Valutazione di Impatto Ambientale

Integrazioni
richieste con nota DVA prot. 22746 del 4/10/2017

ALLEGATO A

Giani, G., Gotta A., Marzano F., Rocca V., 2017 - How to Address Subsidence Evaluation for a Fractured Carbonate Gas Reservoir Through a Multi-disciplinary Approach

Novembre 2017

Geotech Geol Eng
DOI 10.1007/s10706-017-0296-7

ORIGINAL PAPER

How to Address Subsidence Evaluation for a Fractured Carbonate Gas Reservoir Through a Multi-disciplinary Approach

Gian Paolo Giani · Andrea Gotta · Francesco Marzano · Vera Rocca

Received: 14 February 2017 / Accepted: 28 June 2017

Abstract This paper presents and discusses the outcome of a multi-disciplinary study aimed at evaluating ground surface movements which could be potentially induced by the future gas production of a carbonate reservoir located in central Italy. Thanks to both good quality and quantity of data (i.e. seismic surveys, well logs, petrophysical data, PVT-PressureVolumeTemperature-fluid data, geotechnical lab data) the issue was addressed via the set-up of a coupled 3D fluid flow and mechanical model based on the preliminary definition of a 3D structural and geological model. Because it is a forecast study, no model calibration was possible, consequently a set of sensitivity analyses were performed so as to assess the effect of the most critical parameters on subsidence evolution. The 3D FEM (Finite Element Method) mechanical model was set up by adopting an elasto-plastic constitutive law. The model was populated via the integration of data from different sources at different scales (i.e. lab tests, in situ acquisition, literature) and data interpretation adopting a traditional rock mechanics approach, in other words Bieniawski classification and the Barton classification. The obtained strength and deformation parameters depend on the Hoek and Brown criterion and the GSI classification application.

Keywords Subsidence evaluation · Carbonate gas reservoir · 3D FEM mechanical model · Coupled fluid flow–mechanical approach

1 Introduction

It is well-known that subsidence can be caused by both long-term natural processes and by anthropogenic activities, but the effects occur at different time and spatial scales. In particular, ground movements induced by hydrocarbon reservoir exploitation usually evolve in a given period of time and are related to a bounded area. As good practice and in agreement with a sustainable oil industry approach (Rocca and Viberti 2013) the time-evolution of induced subsidence phenomena is forecast (both in terms of magnitude of the displacement and extension of the involved area) so as to assess its potential impact on existing constructions and infrastructures, especially on highly urbanized areas. Research and applied studies have been using analytical and semi-analytical approaches (Streit and Hillis 2004; Soltanzadeh and Hawkes 2009; Selvadurai 2009; Mathias et al. 2010; Rohmer and Bouc 2010)

G. P. Giani
GEAM, Land Resources and Environment Association, C/o Politecnico di Torino, Corso Duca Degli Abruzzi 24, 10129 Turin, Italy

A. Gotta · F. Marzano · V. Rocca (✉)
Department of DIATI, Faculty of Engineering, Politecnico di Torino, Corso Duca Degli Abruzzi 24, 10129 Turin, Italy
e-mail: vera.rocca@polito.it

Published online: 08 July 2017

as well as numerical multiphase coupled techniques (Dean et al. 2003, 2006; Settari and Walters 2001; Rutqvist et al. 2002; Benetatos et al., 2015; Codegone et al. 2016) for subsidence evaluation purposes.

No matter the approach, the rock volume that must be carefully analyzed and characterized, from a petrophysical and a geotechnical standpoints, is that of the hydrocarbon-bearing formation and its cap rock. In fact, ground movements due to fluid exploitation are mainly affected by the stress–strain behavior of the hydrocarbon bearing formations and, secondly, by the stress–strain behavior of the cap rock. Conversely, the overburden formations up to the surface mainly undergo rigid movements. As a consequence, a reliable subsidence prediction requires an appropriate geotechnical characterization of the reservoir and the cap rock.

It is common practice to retrieve cores from the reservoir and cap rock sequences to evaluate the deformation and strength parameters via lab tests. Core analyses provide very accurate yet local information so they fail to capture the large-scale heterogeneities which affect the rock deformation behavior as a whole. An extensive geotechnical coverage of the deformation properties can be obtained by both additional information from well logs adjusted to core data and suitable data analysis and interpretation according to the best practice of rock mechanics.

This paper presents and discusses the outcome of a multi-disciplinary study aimed at evaluating ground surface movements which could be potentially induced by the future gas production of a fractured Carbonate reservoir located in central Italy. The issue was addressed via the set-up of a coupled 3D fluid flow and mechanical model based on the preliminary definition of a 3D structural and geological model. Because it is a forecast study, no model calibration was possible, consequently a set of forecast simulations were performed to evaluate subsidence evolution according to different dynamic scenarios (related to different aquifer strengths and so pressure support) and different deformation parameters.

The time-domain of the analysis included not only the production period, when pore pressure reduction induced land subsidence, but also the system re-pressurization phase due to aquifer support (and consequent land uplift) until a new equilibrium was achieved.

Particular attention was paid to model rock mechanics characterization: data from different sources at different scales (i.e., lab tests, in situ acquisition, literature) was integrated and interpreted adopting a traditional rock mechanics approach, in other words the Bieniawski classification and the Barton classification.

2 Geological Setting

The gas field object of this study is located in central Italy, 36 km south-east of Chieti (Fig. 1).

The Italian peninsula and its surrounding marine areas went through a complex geological evolution since the end of the Paleozoic. The architecture of the Apennine fold-and-thrust belt is the result of this evolution (Cazzola et al. 2011).

The ENE-verging Apennine belt developed during the Neogene and migrated eastward, as documented by the age of the syntectonic siliciclastic foredeep and piggyback deposits (Ricci Lucchi 1986; Boccaletti et al. 1990; Cosentino et al. 2010; Vezzani et al. 2010). In this geodynamical setting several petroleum systems have developed, some of which have a primary economic significance (Bertello et al. 2010).

During the Neogene-Quaternary, in the Central Apennines, pre-orogenic normal faults related to the Mesozoic rift were reactivated with compressional kinematics generating positive structures (e.g. Maiella and Casoli-Bomba) (Fig. 1). The Casoli-Bomba structure can be interpreted as a pop-up structure (Patacca et al. 2008) or as a shortcut structure (Calamita et al. 2009, 2011) resulting from normal faults inversion.

The reservoir under analysis (average depth about 1000 m ssl) is hosted in the southern portion of the buried Casoli-Bomba structure (Fig. 1b). From a lithological point of view the reservoir is made up of limestones belonging to the Bolognano Formation (upper Mioc.) and to the underlying undifferentiated carbonate platform units (Cret.-Mioc.) (Apulia-Adriatic deformed units) (Calamita et al. 2009; Vezzani et al. 2010).

The trap is a N-S trending asymmetric anticline associated to a NNW-SSE striking backthrust verging toward SW. The aquifer connected to the reservoir extends to the N and is bounded in the other directions by two sealing faults. They correspond to the SW-

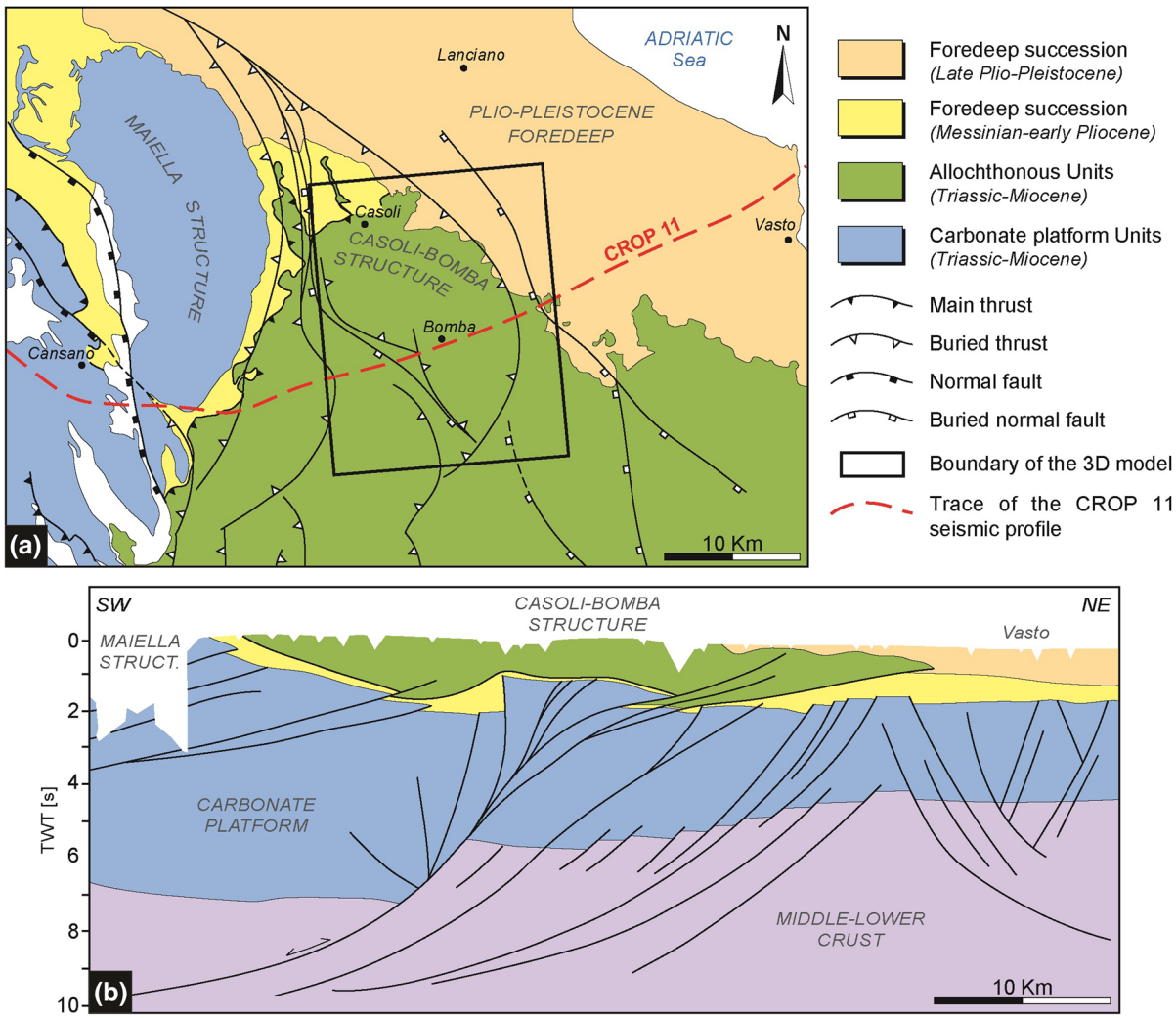

Fig. 1 **a** Simplified structural map of the central-southern Apennine around the modeled area. **b** *Line drawing* of the eastern part of the CROP 11 seismic profile (modified from Calamita et al. 2009)

verging backthrust and to an E-verging thrust, respectively.

The cap rock which seals the reservoir is a continuous layer made up of shaly marl (Bolognano Formation) with an average thickness of 20–25 m.

3 Workflow for the Coupled Analysis

The numerical coupled approach adopted in this study is based on the integration of both rock mechanics and petroleum engineering principles.

The study was developed via the set-up of three different numerical models, each one dedicated to a specific domain of investigation (Cancelliere et al. 2014): (1) the 3D geological model provided the structural and stratigraphic representation of the volume under analysis; (2) the 3D FDM (Finite Difference Method) model simulated the pressure sink propagation into the reservoir and surroundings according to different aquifer support scenarios and (3) the 3D FEM (Finite Element Method) rock mechanics model forecast the formation stress–strain behavior (and its effect in terms of subsidence evolution) induced by fluid pressure change.

The interconnection between fluid flow phenomena and porous media deformations was reproduced adopting the one-way coupling methodology.

According to this approach, the formation stress–strain evolution was determined on the basis of the pore pressure variations, yet the pressure field was supposed to be independent from the induced rock deformations. As discussed in the literature, the one-way coupling approach can adequately capture the interaction between reservoir depletion and compaction (Settari and Maurits 1998; Settari and Walters 2001; Dean et al. 2003).

Eventually, the effects of the system main uncertainties on subsidence evolution were assessed via the sensitivity analysis approach. In particular, from a fluid flow standpoint, different aquifer strengths and consequently different pressure supports were simulated; from a mechanical standpoint, both static and dynamic elastic moduli were used to characterize the system.

3.1 Geological Model Set-Up

A 3D geological model at regional scale was set up to target the subsidence analysis purpose. The model adequately reproduced the key stratigraphic and structural features in the domain of investigation (the reservoir, its surrounding formation and the overburden up to the surface). Based on preliminary sensitivity analyses, the extension of the model (26 × 20 km^2 horizontally, 5 km vertically) (Fig. 2) was deemed suitable for a correct description of subsidence evolution, ensuring undisturbed boundary conditions and avoiding numerical instability issues during rock mechanics simulation. Furthermore, the adopted tartan gridding technique provided good compromise between computational time and geological representativeness of the volume mainly involved by the phenomena under analysis.

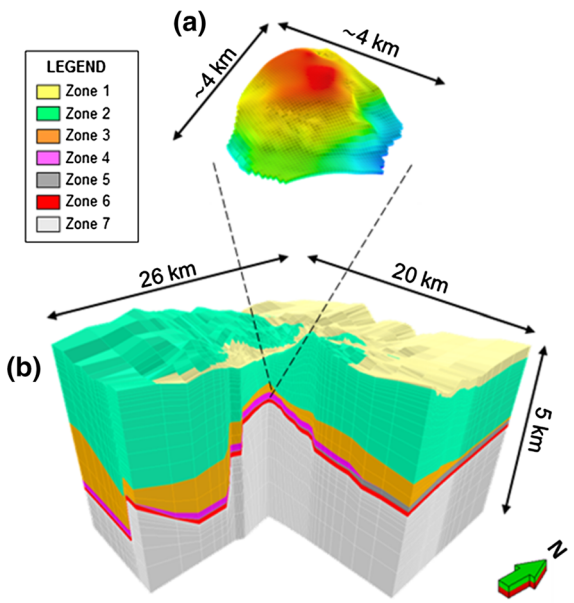

Fig. 2 Reservoir model (**a**) and regional model encompassing it (**b**). For the description of the zones see Table 1

Table 1 summarizes the stratigraphic zonation of the model and the vertical discretization of the 3D grid. The available seismic surveys provided maps and faults at reservoir scale for the structural model definition (Fig. 3).

Furthermore, the overall regional stratigraphy (Table 1) of the investigated area was inferred from the integrated analysis of the seismic data and the composite well logs (at 1:1000 scale) available for 22 wells (UNMIG—Ufficio Nazionale Minerario per gli Idrocarburi e le Georisorse). The 22 wells comprise the 2 wells which targeted the reservoir and the wells drilled in the surrounding area. The literature analysis also provided useful geological information (Festa et al. 2006; Patacca et al. 2008; Calamita et al. 2009, 2011).

According to the analysis of the available data the 3D model was subdivided into 7 main lithostratigraphic units (Zone 1–7) shown in Fig. 2 and described in Table 1. Well correlation provided a more detailed stratigraphic zonation of the carbonate reservoir sequence (Table 1). The identified rock units are characterized by quite homogeneous lithology and geotechnical properties.

3.2 Fluid Flow Model Set-Up

Fluid flow was simulated in the central portion of the regional model just because it was first assessed that production operations induce fluid pressure variations only in a limited portion of the overall model, whereas elsewhere the fluid pressure distribution remains almost constant and equal to the original one. In fact, the reservoir and its surrounding aquifer are dynamically bounded toward E, W and S by two regional sealing faults (Fig. 3), beyond which pressure variations are negligible. In the other direction the 100% water saturated volume affected by pressure variations was constrained by two different aquifer support hypotheses: a medium support and a strong one. In

Table 1 Stratigraphic zonation and vertical discretization of the 3D model

Age	Formation	Lithology	Mean thickness (m)	3D model	
				Zone	Layer
Quaternary	Alluvium and plio-pleistocene foredeep	Sand and clayey sand	20	1	1
Cretaceous–Miocene	Alloctonous (Molise and Sicilidi units)	Marls and calcareous marls with subordinated scaly shale	920	2	2–13
Pliocene	Santerno Fm	Shale and silty shales	230	3	14–15
Late Miocene	Gessoso–Solfifera Fm	Gypsum and gipsy marls	170	4	16–18
Cretaceous–Miocene	Apulia–Adriatic deformed Units (Bolognano Fm and undifferentiated Meso-Cenozoic calcareous successions)	Marly and shaly limestones (cap rock)	25	5	19–20
		Fractured calcarenites and limestones (reservoir)	120	6	21–56
		Limestones and calcarenites	3515	7	57–66

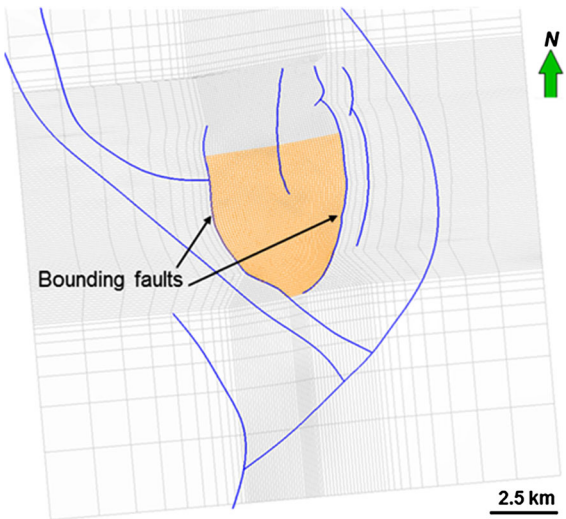

Fig. 3 Top view of 3D grid. The *blue lines* are regional faults; the static/dynamic model grid is *orange*

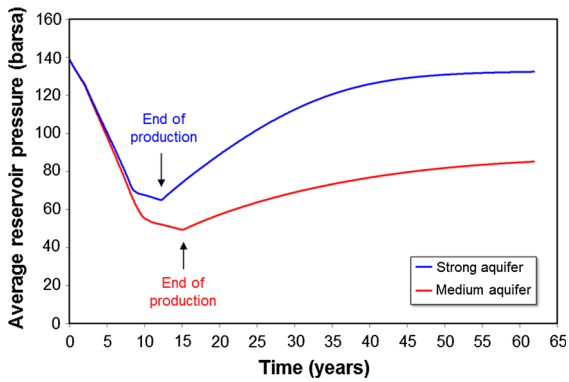

Fig. 4 Time evolution of average reservoir static pressure according to strong and medium aquifer supports

fact, on the basis of both the available study on underground aquifer continuity and the analogy with similar reservoirs already developed, the reservoir under analysis is realistically bounded by an active aquifer. Under a pressure evolution standpoint, this boundary condition corresponds to a pressure support due to water encroaching into the reservoir: it narrows the pressure drop caused by production and induces a system re-pressurization after production. Obviously, the consistency of the aquifer hypotheses will be confirmed by monitored reservoir response (especially in terms of pressure evolution and gas–water contact position) during primary production.

The fluid flow model was set up based on the geological model and all the available petrophysical and fluid properties together with well test data. The initialized dynamic model was then adopted to forecast the spatial distribution and the evolution in time of the pore pressure in the reservoir and in the surroundings for a medium and a strong aquifer hypotheses. After production, dynamic simulations were performed for 45 years so as to describe the new dynamic equilibrium.

These pore pressure maps generated according to the described scenarios were the input of the mechanical analysis. Figure 4 shows the average static

pressure evolution in the reservoir according to the two different scenarios.

3.3 Rock Mechanics Model Set-Up

A 3D FEM model was set up by discretizing the investigated formations in order to carry out a stress–strain analysis. The geological and structural features together with the key formation petrophysical and mechanical properties formed the basis for rock mechanics modelling set up and characterization.

In the initialization phase, the initial pore pressure distribution and the original stress state field were defined for all the investigated volumes according to the available data (i.e.: initial static pressure and well logs). Subsequently, the rock mechanics model was adopted to assess subsidence phenomena according to different scenarios.

Rock mechanics engineering analyses were developed according to the elastic—purely plastic constitutive law and adopting the Mohr–Coulomb failure criteria.

4 Rock Geotechnical Characterization

The modeled volume was subdivided into different materials identified by their mechanical features, which mainly depend on the lithology and on the geological history. Each unit was assumed to be homogeneous and to exhibit an isotropic geomechanic behavior and was defined by assigning initialization, deformation and strength parameters.

The interpretation of the composite logs provided the detailed stratigraphy of the reservoir and the surrounding rock units in the Casoli-Bomba area. The prevailing lithologies in the investigated volume include sand, shale, marl, evaporite (gypsum and gypsy marl), marly limestone, calcarenite and limestone. The reservoir is hosted by fractured limestones and calcarenites and the cap rock consists of unfractured marly limestones.

The available dataset for rock characterization consisted of rock compressibility values from lab analyses for reservoir formation and a set of density + sonic logs. The interpretation of the latter allowed the definition of the dynamic elastic modulus values vs depth. These data were analyzed and interpreted adopting a traditional approach of rock mechanics. Furthermore, they were integrated and extended at model scale with information from the technical literature. Table 2 summarizes the mechanical parameters for model characterization, obtained as discussed later on.

4.1 Geotechnical Parameter Definition

The elastic moduli and the strength parameters (according to the Mohr–Coulomb criterion) were determined via the adoption of the Bieniawski classification together with the Hoek and Brown criterion. In detail, for each formation, except for zones 1, 2 and

Table 2 Mechanical parameters adopted for rock characterization

Layer in 3D model	Class	ν (–)	β (–)	Bulk density (g/cm^3)	σ'_H/σ'_v (–)	σ'_h/σ'_v (–)	Hor. stress azimuth (°)	Vertical stress (°)	Cohesion (bar)	Friction angle (°)
1	1			1.90					2	38
2–3	2			2.30					6	30
4–13	3			2.30					6	30
14–15	4	0.3	1.0	2.30	0.9	0.9	90	90	8	28
16–18	5			2.40					20	25
19–20	6 (*)			2.60					60	39
21–56	7 (**)			2.70					49	37
57–66	8			2.70					100	40

ν, Poisson's coefficient; β, Biot's coefficient; $\sigma_{v'}$, vertical effective stress; $\sigma_{H'}/\sigma_{v'}$, coefficient of maximum horizontal stress; $\sigma_{h'}/\sigma_{v'}$, coefficient of minimum horizontal stress

* Cap rock

** Reservoir

A. CLASSIFICATION PARAMETERS AND THEIR RATINGS									
Parameter			Range of values						
1	Strength of intact rock material	Point-load strength index	>10 MPa	4 - 10 MPa	2 - 4 MPa	1 - 2 MPa	For this low range - uniaxial compressive test is preferred		
		Uniaxial comp. strength	>250 MPa	100 - 250 MPa	50 - 100 MPa	25 - 50 MPa	5 - 25 MPa	1 - 5 MPa	< 1 MPa
	Rating		15	12	7	4	2	1	0
2	Drill core Quality *RQD*		90% - 100%	75% - 90%	50% - 75%	25% - 50%	< 25%		
	Rating		20	17	13	8	3		
3	Spacing of		> 2 m	0.6 - 2 . m	200 - 600 mm	60 - 200 mm	< 60 mm		
	Rating		20	15	10	8	5		
4	Condition of discontinuities (See E)		Very rough surfaces Not continuous No separation Unweathered wall rock	Slightly rough surfaces Separation < 1 mm Slightly weathered walls	Slightly rough surfaces Separation < 1 mm Highly weathered walls	Slickensided surfaces or Gouge < 5 mm thick or Separation 1-5 mm Continuous	Soft gouge >5 mm thick or Separation > 5 mm Continuous		
	Rating		30	25	20	10	0		
5	Groundwater	Inflow per 10 m tunnel length (l/m)	None	< 10	10 - 25	25 - 125	> 125		
		(Joint water press)/ (Major principal σ)	0	< 0.1	0.1, - 0.2	0.2 - 0.5	> 0.5		
		General conditions	Completely dry	Damp	Wet	Dripping	Flowing		
	Rating		15	10	7	4	0		

Fig. 5 Abacus for RMR definition (Bieniawski 1979)

3 (see Table 1), the RMR—Rock Mass Rating (Bieniawski 1973, 1984) was calculated via the abacus of Fig. 5 (Bieniawski 1979).

Subsequently, the GSI—Geological Strength Index was determined according to the following relation:

$$GSI = RMR'_{89} - 5 \quad (1)$$

where RMR'_{89} is evaluated considering drained conditions. The GSI is adopted in the Hoek and Brown (1980a, b) criterion. This criterion (applied via RocLab code ^{TM}RocScience) allows the estimation of the deformation and strength parameters on the base of the following data: rock UCS, mi index (which is a function of the linotype), in situ minimal principal stress and GSI.

Concerning the gas bearing formation, RMR was evaluated assuming the parameter values showed in the abacus reported in Fig. 5 and determined on the basis of available information, such as: FMI log (Formation Microimager) and rock compressibility in the range of 1.3–14 $\times$ 10^{-6} kg/cm^2 from lab analyses (no raw lab data was available).

The obtained RMR equals 72 which corresponds to good quality of the rock mass. The corresponding GSI was 75. On the basis of the GSI value, and considering: a uniaxial compressive strength = 70 MPa, mi = 8 (that corresponding to a micritic limestone, according to Hoek and Brown), an in situ minimum principal stress = 14.5 MPa (which averagely represents the in situ stress state of the reservoir), the application of the Hoek and Brown criterion returned the following values:

- Cohesion 4.99 MPa
- Friction angle 37.14°
- Elastic static modulus of the whole formation, E_S 22.86 GPa

These values represent a good quality limestone, slightly weakened by fractures and discontinuities.

The same workflow was adopted to determine the deformation and the strength parameters for each rock unit reproduced into the model except for the lithologies overlying the evaporitic interval (i.e. zones 1, 2, and 3—Table 1). The results are summarized in Table 3.

Zones 1, 2 and 3 mainly consist of sand, shale and marl. The variation of elastic static moduli E_S of these formations versus depth (Fig. 6) were defined according to the following empirical correlation (Teatini et al. 2011):

$$c_M = 1.370 \times 10^{-2} \times \sigma_V^{-1.135} \quad (2)$$

Table 3 Strength and deformation parameters for evaporites, cap rock, reservoir and basal formation

Lithology	Elastic static modulus (GPa)	Cohesion (MPa)	Friction angle (°)
Vaporite	3.52	2.04	24.53
Cap rock	25.22	6.14	39.32
Reservoir	23.86	4.99	37.14
Bottom Fm	27.11	10.90	40.04

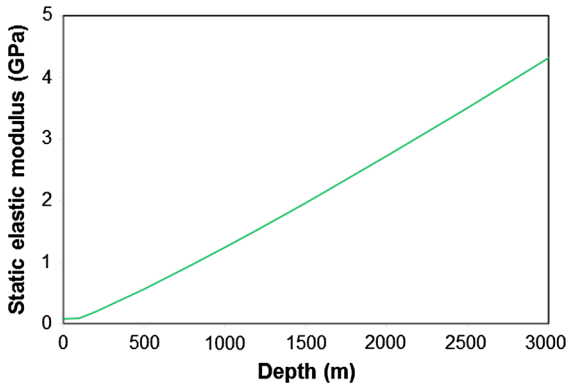

Fig. 6 Static Young's modulus values as a function of depth

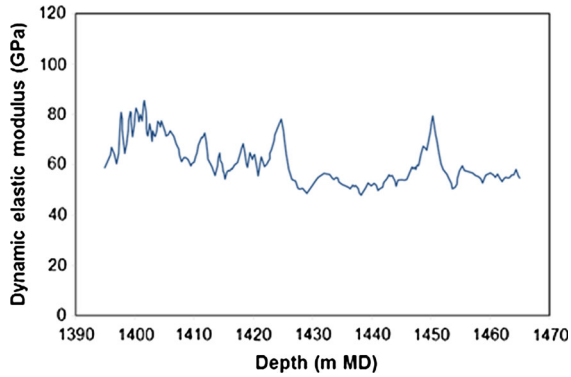

Fig. 7 Dynamic elastic modulus E_D variation versus depth

Equation (2) provides the vertical uniaxial compressibility, c_M, as an exponential function of the vertical effective stress, σ_v. This basin-scale compressibility law was derived from in situ deformation measurements via the radioactive markers. In Teatini's work the investigated formations were silty to fine-grained sandstones, which are similar to the lithologies investigated in this case study. According to their research results, the effect of lithology variation on the elastic modulus values is negligible compared to the influence of depth in shaly-sand formations.

4.2 Elastic Dynamic Moduli

The interpretation of sonic and density logs acquired in the reservoir formation @ Bomba 2 well provided the dynamic elastic modulus values (E_D) as a function of depth. The values shown in Fig. 7 are in substantial agreement with elastic moduli previously evaluated in two other different wells, namely [65.3 +\− 11] GPa and [63.3 +\− 11] GPa.

The dynamic modulus values adopted in the model to characterize the other formations (i.e. cap rock, overburden and underburden) were defined according to a E_D/E_S ratio in the range of 3–4. This choice is supported by the technical literature (Mashinsky 2003; Jiang and Sun 2011; Martínez-Martínez et al. 2012) and it is based on previous authors' experiences: as an example, Codegone et al. (2016) reported dynamic modulus values 3–5 times larger than the static ones, based on experimental data for an Italian gas field within similar lithological contest.

4.3 Elastic Moduli: Definition of Sensitivity Analysis Scenarios

Considering the abovementioned discussion, two analysis scenarios were defined in order to test the impact of deformation parameters on subsidence evolution: static case and dynamic case. Table 4 summarizes the elastic moduli values for each formation adopted during primary production. Furthermore, an extremely conservative case was defined adopting a static elastic modulus equal to 18 GPa in the reservoir.

During the simulation of the re-pressurization phase, assimilated to the in situ unloading state, the elastic moduli were adequately increased to consider formation stiffening due to primary production compaction, in agreement with the technical literature (Baù et al. 2002; Ferronato et al. 2003).

Table 4 Elastic modulus values

Model zones	Static case E_S (GPa)	Dynamic case E_D (GPa)
Alluvium and marine deposit	0.08	0.08
Alloctonous/clay	Linear function of depth	Linear function of depth
Evaporite	3.5	10.5
Cap rock	25	75
Reservoir	23	69
Carbonatic basin	27	81

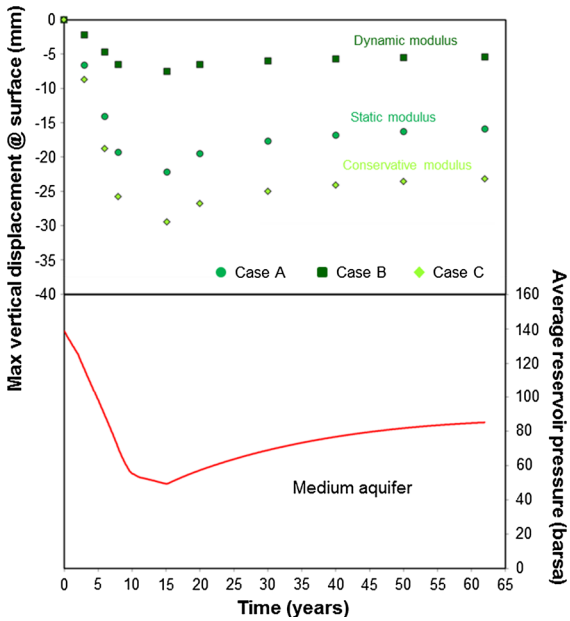

Fig. 8 Medium aquifer: reservoir average pressure time evolution and induced maximum vertical ground movements according to different elastic moduli

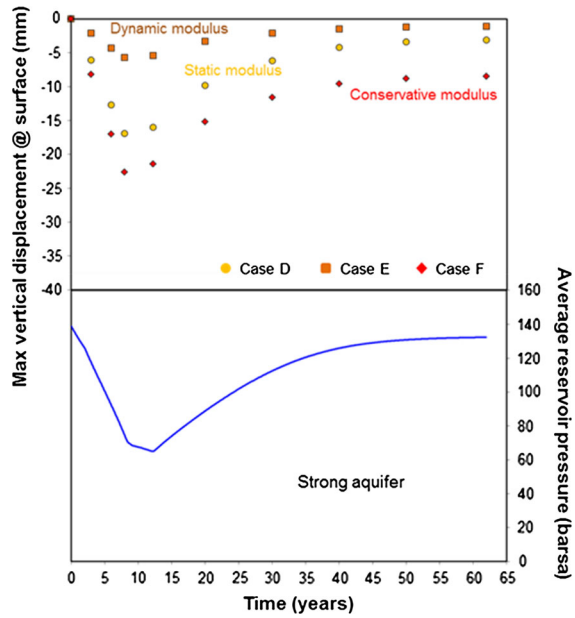

Fig. 9 Strong aquifer: reservoir average pressure time evolution and induced maximum vertical ground movements according to different elastic moduli

4.4 Subsidence Evaluation

The effects of the system main uncertainties on subsidence evolution were assessed via the sensitivity analysis approach and the most important results obtained are reported in this section.

In summary, the six simulated scenarios are:

1. Medium aquifer support

   Case A static elastic modulus values;
   Case B dynamic elastic modulus values;
   Case C conservative elastic modulus values.

2. Strong aquifer support

   Case D static elastic modulus values;
   Case E dynamic elastic modulus values;
   Case F conservative elastic modulus values.

Figures 8 and 9 show, in the cases of medium and strong aquifers respectively, the time evolution of the maximum vertical displacement at ground surface considering the effect of different deformation parameters.

Considering the sensitivities analysis results, from a fluid flow standpoint, less aquifer support (i.e. medium aquifer scenarios), stronger pressure drop during production with consequent increase of induced subsidence. Furthermore, the new fluid flow equilibrium, and consequent ground surface up-lift, is also a function of the aquifer strength.

Regarding the modeling rock mechanics characterization, the best scenario both in terms of the maximum vertical displacement and of the cone radial extension was related to the dynamic elastic modulus assumption, and the worst of the conservative elastic modulus assumption.

Figures 10 and 11, respectively, show the iso-deformation curves (from FEM analysis) at the end of primary production (a) and at the end of simulated period (b) for the worst (i.e. case C) and the best case (case E) scenarios. Furthermore, Table 5 summarizes the results in terms of maximum vertical displacement at the ground level and radius of the subsidence cone (assuming a minimum value of 2 mm) considering both maximum depletion condition and the achievement of a new equilibrium.

In the worst case scenario (case C), the maximum cone extension induced at the end of primary production remains unchanged during the successive re-pressurization period; the effect of the aquifer is appreciated only in terms of vertical displacement modulus attenuation at the end of simulation time. Concerning the best case scenario (case E), the already limited subsidence induced at the end of primary production is totally compensated by pressure support when a new equilibrium is achieved.

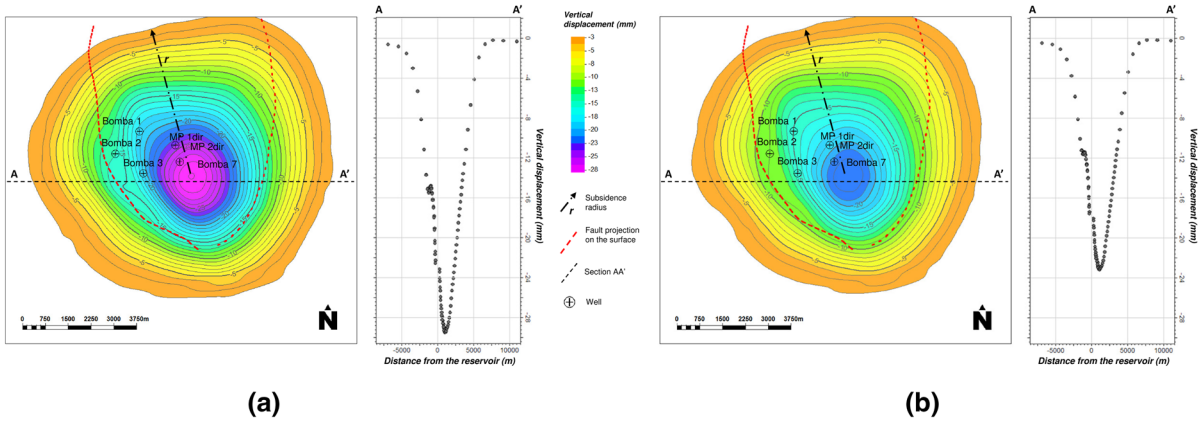

Fig. 10 Case C: subsidence cone at maximum depletion (**a**) and at the end of simulation period (**b**)

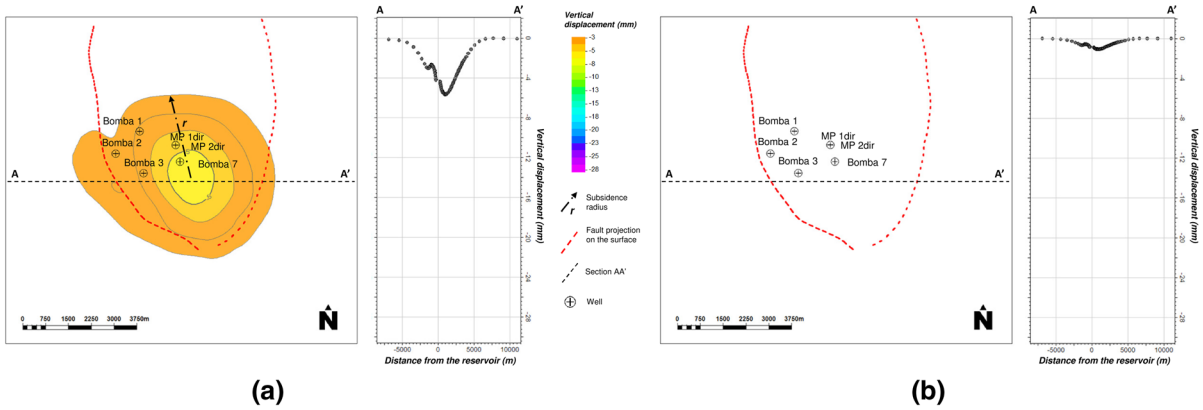

Fig. 11 Case E: subsidence cone at maximum depletion (**a**) and at the end of simulation period (**b**)

Table 5 Results for the worst (case C) and the best (case E) scenarios

Case	Elastic modulus	Aquifer	Max depletion		New equilibrium	
			Max vert displ (mm)	Radius (km)	Max vert displ (mm)	Radius (km)
C	Conserv	Medium	−29.5	5.2	−23.2	5.2
E	Dynamic	Strong	−5.7	2.8	−1.1	–

The stress path induced by any simulated scenarios never reached the Mohr–Coulomb failure envelope: the induced system stress–strain behavior evolved always in purely elastic domain. Furthermore, because no viscous effects were present neither in the reservoir nor in the cap rock formations, the deformation (and so the displacement) increments were instantly achieved concurrently to the effective stress raises induced by pressure drop. During the re-pressurization phase, aquifer support brought partial or total recovery of the induced subsidence (in the elastic domain).

5 Discussion

One of the main factors that control formation stiffness is strain level, where stiffness parameters may be considered constant (i.e., linear) at very small strains but can be expected to decrease from the maximum value as strains increase above this level (Fig. 12) (Abdulhadi and Barghouthi 2012).

Recent research (Descamps et al. 2011; Abdulhadi and Barghouthi 2012; Jiang and Sun 2011) has focused on the experimental definition of the deformation threshold between dynamic and static elastic moduli. In particular, Abdulhadi et al. (2012) investigated the non-linear deformation curves (shear modulus reduction curve, G, vs. log of shear strain curves, γ) via resonant column tests on intact carbonate specimens (comparable to the reservoir formation under analysis): the smooth transition between dynamic and static shear modulus starts for shear strain in the order of $10^{-4}\%$.

According to the simulation results of the case study, the average shear strain induced into the cap rock and the reservoir formations at the end of primary production ranges in the order of $2 \times 10^{-5}\%$, with maximum value of about 6–8 $\times$ $10^{-5}\%$ (achieved for the worst case scenario: see Fig. 13). Consequently, the physical stress–strain deformation behavior of reservoir rock should be realistically represented by the dynamic modulus value. On the other hand, simulation results according to static elastic values bounded the variation range of subsidence phenomena. In particular, the conservative case corresponds to an engineering approach: the penalty in the elastic modulus corresponds to the introduction of a safety factor on the result, expressed in terms of subsidence.

During future reservoir exploitation and subsequent re-equilibration period once production stops, the system behavior will be monitored in terms of time evolution of ground movements and of produced fluid volumes and consequent reservoir pressure variation. The acquired data will allow the calibration of both fluid-flow (considering, for example, the assisted history match option (Cancelliere et al. 2011; Verga et al. 2013)), and rock mechanics models. The calibrated parameters will be suitably adopted for forecasting the remaining future reservoir response.

In the case of the reservoir under analysis, a GPS system is already present and the data, acquired in the 2007–2009 period, has highlighted an existing ground surface movement due to natural processes. These seasonal vertical surface oscillations were in the order of 25 mm and they could be realistically ascribed to a

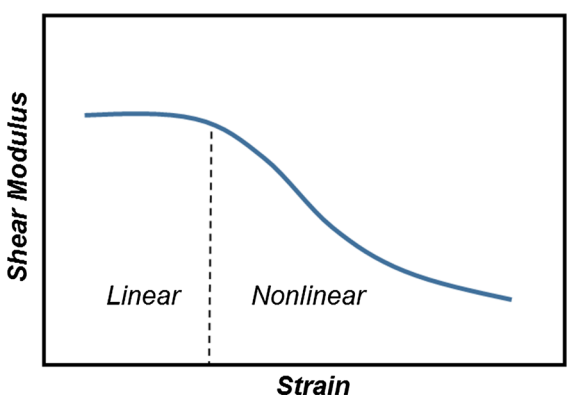

Fig. 12 Qualitatively variation of Shear Modulus versus Strain (Abdulhadi and Barghouthi 2012, modified)

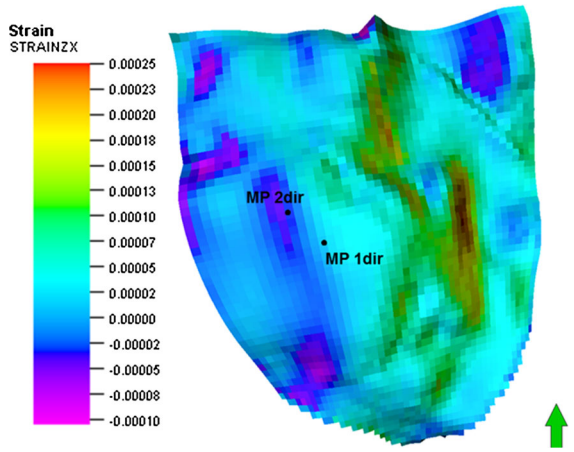

Fig. 13 The worst case scenario—C: Iso-deformation curves (shear deformation) γ_{zx} in the reservoir @ maximum depletion

seasonal temperature variation. According to simulation results, the average annual ground displacement due to production should be in the range of [0.5–2.8] mm/year, one order of magnitude lower than the existing natural annual excursion (50 mm).

6 Conclusion

This paper described the application of an integrated static-dynamic and mechanical workflow to investigate the ground surface movement potentially induced by the future gas production from a carbonate reservoir located in central Italy.

The 3D FEM (Finite Element Method) rock mechanics model was set up by adopting an elasto-plastic constitutive law. The elastic moduli and the strength parameters (according to Mohr–Coulomb criterion) were determined by interpreting the available data (lab tests and in situ log data) via the Bieniawski classification together with the Hoek and Brown criterion.

Because no model calibration was possible, a set of sensitivity analyses were performed so as to assess the effect of the most uncertain and/or critical parameters on subsidence evolution: concerning dynamic aspects, different aquifer strengths and consequent pressure support were tested; regarding rock mechanics aspects, different deformation parameters were adopted. The results allowed the quantification of the worst and the best (and the most likely) subsidence scenarios. It is important to stress that, according to simulation results, the average annual ground displacement due to production should be in the range of [0.5–2.8] mm/year, one order of magnitude lower than the existing natural annual excursion (50 mm) monitored via GPS system.

Acknowledgements The authors wish to thank CMI Energia SpA for permission to publish the data presented in this paper.

References

Abdulhadi N, Barghouthi A (2012) Measurement of stiffness of rock from laboratory and field tests. In: Proceedings of the 5th Jordanian international civil engineering conference, 2012

Baù D, Ferronato M, Gambolati G, Teatini P (2002) Basin-scale compressibility of the Northern Adriatic by the radioactive marker technique. Géotechnique 52(8):605–616. doi:10.1680/geot.2002.52.8.605

Benetatos C, Rocca V, Sacchi Q, Verga F (2015) How to approach subsidence evaluation for marginal fields: a case History. Open Petrol Eng J 8:214–234

Bertello F, Fantoni R, Franciosi R, Gatti V, Ghielmi M, Pugliese A (2010) From thrust-and-fold belt to foreland; hydrocarbon occurrences in Italy. In: Vining BA, Pickering SC (eds) Petroleum geology, from mature basins to new frontiers, proceedings of the 7th petroleum geology conference: petroleum geology conference proceedings, vol 7, pp 113–126

Bieniawski ZT (1973) Engineering classification of jointed rock masses. Trans S Afr Inst Civ Eng 15:335–344

Bieniawski ZT (1979) The geomechanical classification in rock engineering applications. In: Proceedings of the 4th international congress rock mechanics, Montreux, Switzerland, 2–8 September 1979

Bieniawski ZT (1984) Rock mechanics design in mining and tunnelling. Balkema, Rotterdam

Boccaletti M, Calamita F, Deiana G, Gelati R, Massari F, Moratti G, Ricci Lucchi F (1990) Migrating foredeep-thrust belt systems in the northern Apennines and southern Alps. Palaeog Palaeocl Palaeoec 77:41–50

Calamita F, Esestime P, Paltrinieri W, Scisciani V, Tavarnelli E (2009) Structural inheritance of pre-and syn-orogenic normal faults on the arcuate geometry of Pliocene-Quaternary thrust: examples from Central and Southern Apennine chain. Ital J Geosci 128:381–394

Calamita F, Satolli S, Scisciani V, Esestime P, Pace P (2011) Contrasting styles of fault reactivation in curved orogenic belts: examples from the Central Apennines (Italy). Geol Soc Am Bull 123:1097–1111. doi:10.1130/B30276.1

Cancelliere M, Verga F, Viberti D (2011) Benefits and limitation of assisted history matching. SPE 146278. In: Offshore Europe, oil and gas conference and exhibition. 6–8 September 2011. Aberdeen (UK). ISSN: 9781613991381

Cancelliere M, Viberti D, Verga F (2014) A step forward to closing the loop between static and dynamic reservoir modeling. Oil Gas Sci Technol 69(7):1201–1225. doi:10.2516/ogst/2013178

Cazzola A, Fantoni R, Franciosi R, Gatti V, Ghielmi M, Pugliese A (2011) From thrust and fold belt to foreland basins: hydrocarbon exploration in Italy. In: Extended abstract for oral presentation at AAPG international conference and exhibition, Milan, Italy, 3–26 October 2011, p 6

Codegone G, Rocca V, Verga F, Coti C (2016) Source of the document geotechnical and geological engineering. Geotech Eng Eng Geol 34(6):1749–1763

Cosentino D, Cipollari P, Marsili P, Scrocca D (2010) Geology of the central Apennines: a regional review. J Virt Expl. doi:10.3809/jvirtex.2009.00223

Dean RH, Gai X, Stone CM, Minkoff SE (2003) A comparison of techniques for coupling porous flow and geomechanics. In: Proceedings of the SPE reservoir simulation symposium, Houston, Texas, USA, 3–5 February 2003. doi:10.2118/79709-MS

Dean RH, Gai X, Stone CM, Minkoff SE (2006) A comparison of techniques for coupling porous flow and geomechanics. SPE J 11(01):132–140. doi:10.2118/79709-PA

Descamps F, Tahibangu JP, Ramos da Silva M, Schroeder C, Verbrugge JC (2011) Behaviour of carbonated rocks under true triaxial compression. In: 12th ISRM congress, Beijing, China, 16–21 October 2011

Ferronato M, Gambolati G, Teatini P (2003) Unloading-reloading uniaxial compressibility of deep reservoirs by marker measurements. In: Proceedings of the 11th international FIG symposium on deformation measurements, Santorini Island, Greece, pp 341–346

Festa A, Ghisetti F, Vezzani L (2006) Carta Geologica del Molise, scala 1:100 000, Note Illustrative. Nichelino (TO), Litografia Geda, pp 104, ISBN 88-902635-0-4

Hoek E, Brown ET (1980a) Underground excavations in rock. Instn Min Metall, London

Hoek E, Brown ET (1980b) Empirical strength criterion for rock masses. J Geotech Eng Div 106(GT9):1013–1035

Jiang J, Sun J (2011) Comparative study of static and dynamic parameters of rock for the Xishan Rock Cliff Statue. J Zhejiang Univ-Sci A 12(10):771–781

Martínez-Martínez J, Benavente D, García-del-Cura MA (2012) Comparison of the static and dynamic elastic modulus in carbonate rocks. Bull Eng Geol Environ 71:263–268. doi:10.1007/s10064-011-0399-y

Mashinsky EI (2003) Differences between static and dynamic elastic moduli of rocks: physical causes. Russ Geol Geophys 44(9):953–959

Mathias SA, Hardisty PE, Trudell MR, Zimmerman RW (2010) Screening and selection of sites for CO_2 sequestration based on pressure buildup. Int J Greenb Gas Control 4:108–109

National Office for Hydrocarbons and Mining georesources of Italy (UNMIG) http://unmig.sviluppoeconomico.gov.it/. Accessed Nov 2015

Patacca E, Scandone P, Di Luzio E, Cavinato GP, Parotto M (2008) Structural architecture of the central Apennines: interpretation of the CROP 11 seismic profile from the Adriatic coast to the orographic divide. Tectonics 27(TC3006):1–36. doi:10.1029/2005TC001917

Ricci Lucchi F (1986) The oligocene to recent foreland basins of the northern Apennines. Int Ass Sed Spec Publ 8:105–139

Rocca V, Viberti D (2013) Environmental sustainability of oil industry. Am J Environ Sci 9:210–217. doi:10.3844/ajessp.2013.210.217

Rohmer J, Bouc O (2010) A response surface methodology to address uncertainties in cap rock failure assessment for CO_2 geological storage in deep aquifers. Int J Greenh Gas Control 4(2):198–208. doi:10.1016/j.ijggc.2009.12.001

Rutqvist J, Wu Y-S, Tsang C-F, Bodvarsson GA (2002) A modeling approach for analysis of coupled multiphase fluid flow, heat transfer, and deformation in fractured porous rock. Int J Rock Mech Min Sci 39(4):429–442. doi:10.1016/S1365-1609(02)00022-9

Selvadurai APS (2009) Heave of a surficial rock layer due to pressures generated by injected fluids. Geophys Res Lett. doi:10.1029/2009GL038187

Settari A, Maurits FM (1998) A coupled reservoir and geomechanical simulation system. SPE J 3(03):219–226. doi:10.2118/50939-PA

Settari A, Walters DA (2001) Advances in coupled geomechanical and reservoir modeling with applications to reservoir compaction. SPE J 6(03):334–342. doi:10.2118/74142-PA

Soltanzadeh H, Hawkes CD (2009) Assessing fault reactivation tendency within and surrounding porous reservoirs during fluid production or injection. Int J Rock Mech Min Sci 46(1):1–7. doi:10.1016/j.ijrmms.2008.03.008

Streit JE, Hillis RR (2004) Estimating fault stability and sustainable fluid pressures for underground storage of CO_2 in porous rock. Energy 29(9–10):1445–1456. doi:10.1016/j.energy.2004.03.078

Teatini P, Castelletto N, Ferronato M, Gambolati G, Janna C, Cairo E, Marzorati D, Colombo D, Ferretti A, Bagliani A, Bottazzi F (2011) Geomechanical response to seasonal gas storage in depleted reservoirs: a case study in the Po River basin, Italy. J Geophys Res. doi:10.1029/2010JF001793

Verga F, Cancelliere M, Viberti D (2013) Improved application of assisted history matching techniques. J Petrol Sci Eng 109:327–347. doi:10.1016/j.petrol.2013.04.021

Vezzani L, Festa A, Ghisetti FC (2010) Geology and tectonic evolution of the central– southern Apennines, Italy. Geol Soc Am Spec Pap 469:1–58